



Estimation of Slip Ratios for Pressure Drop Calculations in Geothermal wells

Póra Hlín Þórisdóttir



Faculty of Industrial Engineering, Mechanical Engineering and
Computer Science
University of Iceland
2013

ESTIMATION OF SLIP RATIOS FOR PRESSURE DROP CALCULATIONS IN GEOTHERMAL WELLS

Póra Hlín Þórisdóttir

30 ECTS thesis submitted in partial fulfillment of a
Magister Scientiarum degree in Mechanical Engineering

Advisors

Halldór Pálsson

Magnús Þór Jónsson

Faculty Representative

Einar Jón Ásbjörnsson

Faculty of Industrial Engineering, Mechanical Engineering and Computer
Science

School of Engineering and Natural Sciences

University of Iceland

Reykjavik, January 2013

Estimation of Slip Ratios for Pressure Drop Calculations in Geothermal wells
Pressure Drop Calculations in Geothermal Wells
30 ECTS thesis submitted in partial fulfillment of a M.Sc. degree in Mechanical Engineering

Copyright © 2013 Þóra Hlín Þórisdóttir
All rights reserved

Faculty of Industrial Engineering, Mechanical Engineering and Computer Science
School of Engineering and Natural Sciences
University of Iceland
VRII, Hjarðarhaga 2-7
107, Reykjavik, Reykjavik
Iceland

Telephone: 525 4000

Bibliographic information:

Þóra Hlín Þórisdóttir, 2013, Estimation of Slip Ratios for Pressure Drop Calculations in Geothermal wells, M.Sc. thesis, Faculty of Industrial Engineering, Mechanical Engineering and Computer Science, University of Iceland.

Printing: Háskólaprent, Fálkagata 2, 107 Reykjavík
Reykjavik, Iceland, January 2013

Abstract

The goal of this project is to estimate a correlation of slip ratio between gas- and liquid velocity in a two phase flow in a geothermal well. Initially, a model which calculates pressure drop from the bottom to the well top in a geothermal well was developed in Matlab. Then measured data of pressure and depth, which was provided by Orkuveita Reykjavíkur and HS Energy was used to evaluate the models accuracy and use to make a correlation of the slip ratio. In addition 6 previously known void fraction models were tested to see how they fitted according to the measurement data. The result was that due insufficient accuracy of the measurements, a new model could not be developed. However this thesis concludes that a model that assumes no difference in velocity between the liquid and gas phase, is the best for this application until better measured data can be obtained. Based on these conclusions it can be recommended that more accuracy should be introduced in the measurement process, such as gathering all the data at the same time. Better measuring equipment and techniques could contribute to the development of better correlations which could be used to better predict pressure drop more accurately.

Útdráttur

Tilgangurinn með verkefninu er að búa til reynsluformúlu fyrir hraðahlutfall gass- og vökvafasa í tvífasaflæði í jarðhitaborholum. Byrjað var á því að búa til líkan sem reiknar þrýstifall í borholum í Matlab. Gögn úr borholumælingum eru fengin hjá Orkuveitu Reykjavíkur og HS orku. Gögnin átti að nota til að meta nákvæmni líkansins og nýta niðurstöðurnar til að búa til reynsluformúlu fyrir hraðahlutfallið. Að auki voru 6 þekktar reynsluformúlur fyrir rúmhlutfall gufu athugaðar til þess að skera úr um hvort að þær myndu skila betri niðurstöðum. Sú var ekki raunin en ein af niðurstöðum þessarar athugunar er að mælt er með að líkanið sem gerir ráð fyrir sama hraða vatns og gufu (e. no slip model) sé notað þar sem það gaf minnsta skekkju miðað við gögnin. Mælt er með því að nákvæmni sé aukin í mæliferlinu sjálfu, t.d. að taka allar mælingar á sama tíma og jafnvel uppfæra búnaðinn sem notaður er til verksins, að öðrum kosti verður ekki hægt að gera betrubætur á þeim líkönum sem notuð eru til að reikna þrýstifall í jarðhitaborholum.

Contents

List of Figures	ix
Nomenclature	xii
Acknowledgments	xv
1 Introduction	1
2 Geothermal Wells and Two Phase Flow	3
2.1 Two Phase Flow	4
2.2 Two Phase Flow Modeling	5
3 Modeling Method	7
3.1 Thermodynamic properties	8
3.2 Single Phase Flow	8
3.2.1 The continuity equation	9
3.2.2 The energy equation	9
3.2.3 The momentum equation	9
3.2.4 A system of equations	10
3.3 Two Phase Flow	10
3.3.1 The continuity equation	11
3.3.2 The energy equation	11
3.3.3 Momentum equation	12
3.3.4 A system of equations	12
3.4 Slip ratio and void fraction correlations	13
3.5 Friction factor	14
3.6 Friction correction factors	15
3.7 Numerical Integration	16
4 Measured data	17
4.0.1 Mass Flow	17
4.1 Data source	19
4.2 Data	20
5 Results	21
5.1 Comparison of different flow models for each well	21

Contents

5.2	Well head pressure and its sensitivity to changes on slip ratio	25
5.3	Slip ratio calculation on different depths in the well	28
6	Conclusions	31
	Bibliography	33

List of Figures

2.1	Casing program for a typical geothermal well.	4
5.1	Simulations of wells HE-5 (left) and HE-20 (right) from the bottom of the production casing to the well top.	22
5.2	Simulations of wells HE-44 (left) and HE-48 (right) from the bottom of the production casing to the well top.	23
5.3	Simulations of wells Rn-11 (left) and Rn-12 (right) from the bottom of the production casing to the well top. In addition to the simulation results and measurement a data reading error was evaluated due to data reading accuracy on the graphs provided by HS energy. The error was estimated as ± 1 bar and ± 10 m	24
5.4	Simulations of wells SV-21 from the bottom of the production casing to the well top. In addition to the simulation results and measurement a data reading error was evaluated due to data reading accuracy on the graphs provided by HS energy. The error was estimated as ± 1 bar and ± 10 m	25
5.5	Simulated well head pressure changes when the slip ratio input value is changed for wells HE-5 (left) and HE-20 (right). The red line represents the simulated value of wellhead pressure, the blue line is value for measured well head pressure and the blue dotted lines represent the measurement uncertainty evaluated as ± 1 bar for each \pm m.	26
5.6	Simulated well head pressure changes when the slip ratio input value is changed for wells HE-44 (left) and HE-48 (right). The red line represents the simulated value of wellhead pressure, the blue line is value for measured well head pressure and the blue dotted lines represent the measurement uncertainty evaluated as ± 1 bar for each \pm m.	26

LIST OF FIGURES

- 5.7 Simulated well head pressure changes when the slip ratio input value is changed for wells RN-11 (left) and RN-12 (right). The red line represents the simulated value of wellhead pressure, the blue line is value for measured well head pressure and the blue dotted lines represent the measurement uncertainty evaluated as ± 1 bar for each \pm m. 27
- 5.8 Simulated well head pressure changes when the slip ratio input value is changed for well SV-21. The red line represents the simulated value of wellhead pressure, the blue line is value for measured well head pressure and the blue dotted lines represent the measurement uncertainty evaluated as ± 1 bar for each \pm m. 27
- 5.9 Calculations of slip ratio at known locations in the wells where the well head pressure is known. 28
- 5.10 The figure illustrates the effects the measured input value of mass flow on well head pressure calculations on well SV-21. When the mass flow changes by 10%, the well head pressure changes by 1-2%. . 29

Nomenclature

A	Total are of a pipe	[m ²]
A_g	Area of a pipe where only gas exists	[m ²]
A_l	Area of a pipe where only liquid exists	[m ²]
CT	Tracer concentration	
d	Inner diameter of a pipe	[m]
E	Dimensionless factor	
F	Dimensionless factor	
f	Friction factor	
Fr	Froude factor	
G	Mass flux	[kg · m ² /s]
g	Gravitational acceleration	[m/s ²]
H	Dimensionless factor	
h	Enthalpy	[kJ/kg]
h_g	Enthalpy of gas phase in a mixture	[kJ/kg]
h_l	Enthalpy of liquid phase in a mixture	[kJ/kg]
\dot{m}	Mass Flow	[kg/s]
\dot{m}_g	Mass flow steam	[kg/s]
\dot{m}_l	Mass flow liquid	[kg/s]
P	Pressure	[bar]
P_c	Critical pressure	[bar]
S	Slip ratio	
u	Velocity	[m/s]
u_g	Average velocity of gas phase	[m/s]
u_l	Average velocity of liquid phase	[m/s]
Re	Reynolds number	
Re_g	Reynolds number for gas phase	
Re_l	Reynolds number for liquid phase	
T	Temperature	[K]
Q_g	Volume flow of gas phase	[m ³ /s]
Q_l	Volume flow of liquid phase	[m ³ /s]
We	Webber number	
x	Steam quality of mixture	
z	Depth	[m]
α	Void fraction, liquid hold up correlation	
μ_g	Dynamic viscosity of gas phase	[Pa · s]
μ_l	Dynamic viscosity of liquid phase	[Pa · s]

σ	Surface tension,	[N/m]
γ	Simplification parameter	
η	Simplification parameter	
Θ	Friction correction factor	
ρ	Density	[kg/m ³]
ρ_g	Density of gas phase	[kg/m ³]
ρ_l	Density of liquid phase	[kg/m ³]
ν_g	Kinematic viscosity of gas phase	[m ² /s]
ν_l	Kinematic viscosity of liquid phase	[m ² /s]

Acknowledgments

This work would never have been accomplished without the help and support I received from my supervisors; Halldór Pálsson and Magnús Þór Jónsson associate professor and professor at the Faculty of Industrial engineering, mechanical engineering and computer science at the University of Iceland. I would also like to thank Einar Gunnlaugsson and Gunnar Gunnarsson from Reykjavík Energy and Albert Albertsson and Geir Þórólfsson from HS Orka for providing well data for this project. I would also like to thank William S. Harvey visiting professor at Reykjavik University for introducing me to thermodynamics. Most of all I would like to thank my family, especially my son Þórir for being patient. I give all these people me sincerest gratitude.

1 Introduction

Geothermal energy is generated and stored in the Earth. Its utilization is divided into two groups: direct use and electricity production. Direct use includes all areas where the heat in the geothermal fluid can be used directly for example house heating, fish farming and kelp drying. Utilization of geothermal energy in Iceland reaches back to the 10th century where people used water from hot springs to wash and bathe [Haraldsson and Ketilsson, 2010]. High temperature geothermal fluid can be used for electricity production. In such cases the steam is gathered from wells and then expanded in a turbine that provides shaft power to a generator, which converts mechanical energy to electrical energy. In 2009 the electricity production in Iceland from geothermal energy was 4.6 GWh or 27.2% of countries total electricity production [Eggertsson et al, 2010].

Electricity production from geothermal energy can be cost effective compared to other options (coal, gas etc). However the geothermal power plant development has a substantial start up cost where about 30-40% of the cost is involved in well drilling [Ingason and Matthíasson, 2006]. Unfortunately, the drilling cost has increased significantly in the recent years due to an increase in material costs, increased number of directionally drilled wells and drilling under more challenging conditions where the diameters are larger and the wells deeper. This has raised interest in developing more cost effective methods to counter these increases[Thorhallsson, 2008].

The risk in geothermal development is very diverse. The most notable part of it is the financial part. Preliminary investigations on possible geothermal areas are both costly and time consuming and don't always deliver positive results, making investors reluctant to participate in further projects. Another risk aspect is the potential of steam blow outs, distribution of corrosive chemicals and human safety at the locations, which often have surface activity such as upstream of gases such as CO_2 and H_2S . Since the risk in utilization is so high it is important to have good understanding of the main aspects concerning the wells, in this case the flow. Better understanding of the flow can be used to select more appropriate diameters for the wells. By carefully choosing a diameter the drilling cost can be lowered since slim wells are more cost effective than wider wells. Increased knowledge on the flow can be used to predict pressure drop more accurately in the well and give better predictions if changes were to occur on mass flow or pressure in the well.

1 Introduction

The flow in the wells usually consist of two phase flow. The existence of the two phases is a challenge which make computer modeling complicated due to co-existence of turbulence effects and moving boundaries between different phases. The interaction of fluid and gas state can be described with different flow patterns. There are many different methods for evaluating the flow patterns but they depend on transport properties of the two phases, pipe roughness, mass and volume fractions in the pipe and velocity ratio between the two phases. Flow maps are used to indicate which pattern is present. Another factor that makes two phase pressure drop modeling difficult is the fact that gas tends to have greater velocity than the liquid in a gas-liquid flow. This is referred to as a slip ratio, or slippage. The slippage effect makes the mixing fluid properties dependent on the flowing conditions and pipe geometry [Zhao, 2005].

The objective of this thesis is two folded.

1. Make a model that calculates pressure drop in a two phase region in a vertical pipe. Assuming there is no slippage between the phases.
2. Improve the model and comparing them to real measurements from geothermal wells by calculating new slip ratios. Compare the slip ratios corresponding to the measurements in effort to estimate a formula for the slip ratio that could be used to model pressure drop for two phase flow in Icelandic high temperature two phase wells within a suitable error margin.

2 Geothermal Wells and Two Phase Flow

Geothermal wells are usually categorized into low temperature or high temperature wells. The definition of low temperature reaches up to a temperature of 150°C and the high temperature wells are where the temperature exceeds 200°C [Thorhallsson, 2008].

A typical depth of a high temperature well is 1500-3000 meters. Some are straight, others are directionally drilled. The directional drilling is performed to aim better at fault zones, where fluid is more likely to be found and also for environmental purposes. The straight drilling is cheaper but directional drilling can yield better results if targeting faults is a problem and to minimize the visibility of the wells, this concludes that there are many things to be considered beforehand. In the well design process certain steps must be taken to ensure safe drilling and preparation for production of geothermal fluid. The wells are narrow and are lined with 2-5 different casings. The purpose of these casings is to seal out unwanted aquifers, prevent collapse and provide a conduit for the well production. Cement slurry is used to fill the space between each of the casings and the rock. The wells are drilled in steps which are sometimes refereed to as casing programs. After each step a casing is cemented in the well. The casing program are designed for each well and are dependent on its characterization. The most common casing programs are surface casing, anchor casing, production casing and slotted liner. A schematic drawing of a typical casing program can be seen on figure 2.1.

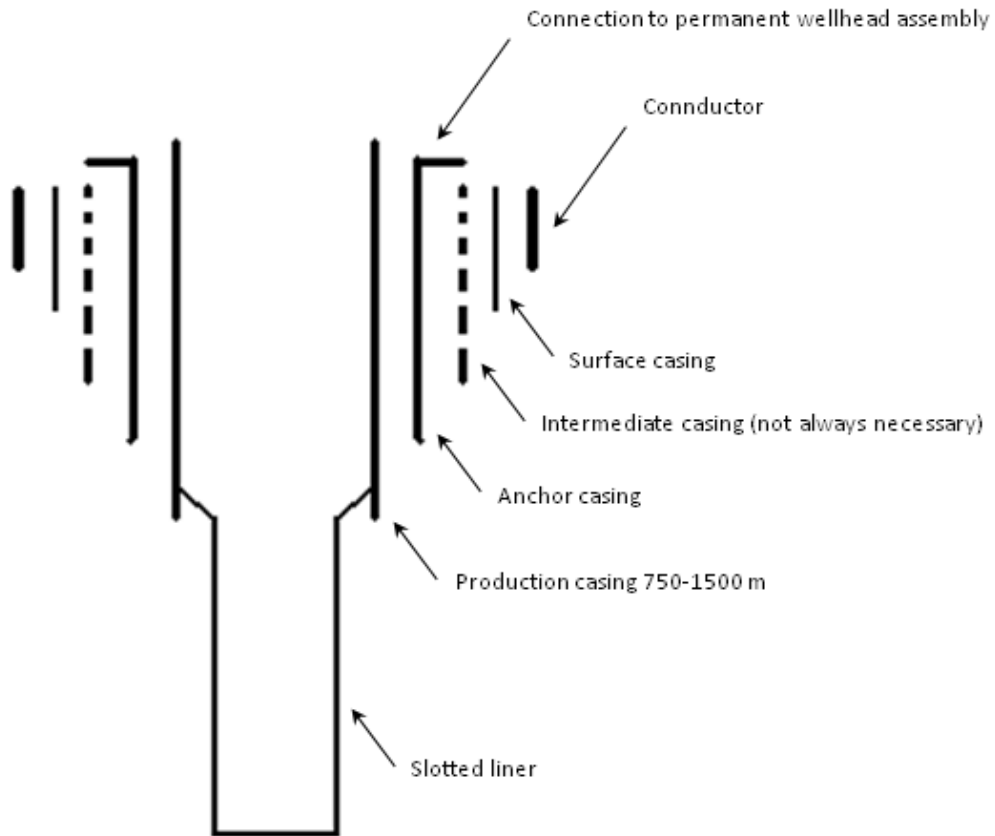


Figure 2.1: Casing program for a typical geothermal well.

2.1 Two Phase Flow

Geothermal wells have to be able to transport energy. In geothermal wells, such as those that are utilized in Iceland, water or brine is the fluid involved in that process. For the purpose of electricity production it is optimal to have dry steam wells however it is more common to have two phase flow where the phases have to be separated to liquid and dry steam before the steam can enter the turbine, any droplets in the steam can cause damage to the equipment. In most two phase geothermal wells the fluid goes through phase change on its way up the well when the liquid starts to boil. This happens due to a drop in pressure on the way up the hole. The area in the well where this change begins is called the flashing zone or flashing horizon [Dipippo, 2009].

2.2 Two Phase Flow Modeling

Two phase flow models are divided into two categories; homogenous flow models and separate flow models. The homogenous models are simpler assuming that the liquid and gas phases move at the same velocity. In the separate flow models it is assumed that different equations are valid for each phase, indicating the different velocity of the two phases. These equations are one form of empirical correlations. The separate flow models are considered to give a more reliable result in the pressure drop calculations. However the empirical correlations are usually correlated inside laboratories at a small scales compared to the size of geothermal wells and do not necessarily give an accurate result when used in well bore simulations.

Pressure drop in a vertical wells is comprised of three factors:

1. Gravity: Pressure changes due to difference in height.
2. Momentum: The different phases do not have the same velocity which causes a change in momentum and thus the pressure.
3. Friction: The friction between the two phases and between the phases and the well walls.

There are three different approaches used to model pressure drop in two phase flow: semi-analytical models, numerical models and empirical models. One of many obstacles in two phase flow modeling is limited knowledge of the subject, therefore all the multi phase flow models depend on empirical correlations up to some extent. The two phase models are usually categorized as:

1. *Empirical models* are simplified relationships based on a series of experiments. However, two phase flow is very sensitive to changes in properties which makes these models only reliable within the range they were correlated on, meaning they were carried out with lab experiments under controlled circumstances [Zhao, 2005].
2. *Semi-analytical methods* or mechanistic methods approximate a physical phenomenon by taking into consideration the most important processes and neglecting other less important effects that add to uncertainty [Zhao, 2005]. These models are made and then fitted to the data and a method of extrapolation is introduced to model other wells.
3. *Numerical method* is the the third form. More details can be driven from numerical analysis methods than any other, such as distribution of the phases, dynamic flow regime transition and turbulence effects. [Zhao, 2005]. In this

2 Geothermal Wells and Two Phase Flow

case numerical integration is used to solve equations 3.22 and 3.5 over the production casings length.

This model is a mixture of the first two types. Some of the input values used in the models are from empirical correlations and the model is fitted to measured data by using the semi-analytic method.

3 Modeling Method

The purpose of this work is to make a model that can be used to predict pressure drop in a two phase region of high temperature geothermal wells in Iceland. The first step is to make a model which treats the two phases having equal velocities, or no slippage. That model is chosen since it is the most simple one. The second step is to compare the model with actual data and calculate the slip ratio which is the ratio between the velocities of the gas and liquid. Compare results of the slip ratio calculations and estimate a correlation that can be used in the improved model.

Two phase flow follows all of the basic laws of fluid mechanics. However the equations are more complicated than for single phase flow since the phases have different properties. One of the aspects of evaluating an empirical model of the well is to have access to accurate data.

Information on well properties:

- Length of production casing
- Inner diameter of production casing
- Fluid properties; enthalpy, temperature, pressure.

For the purpose of this project which is complicated to measure such as wall roughness. In the model it is assumed that walls are smooth.

Other factors which are calculated or estimated from empirical correlations are:

- Flow velocity, fluid and liquid velocity
- Density of both phases
- Dynamic viscosity of both phases

3 Modeling Method

- Surface tension
- Steam quality
- Friction factor

The numerical approaches used in model are introduced in this chapter for both the single- and two phase regions. The method used to simulate flow of water and steam in a vertical circular pipe with a constant diameter. Steady state conditions apply and thus time dependent variations are neglected. It is assumed that the fluid is pure water with well known thermodynamic and transport properties. The equations form a coupled first order set of ordinary differential equations that can be solved either by finite difference methods or integrated from the bottom to the top. The modeling starts at the bottom of the production casing and it is necessary to implement both single-and two-phase equations and correlations in the model since flashing can occur within the casing. The governing equations are expressed as proposed by [Pálsson, 2011a].

3.1 Thermodynamic properties

Thermodynamic properties of the fluid are calculated using The International Association for the Properties of Water and Steam (IAPWS) standards. The interpolations are carried out in REFPROP. These primary parameters include saturation properties for both water and steam state; enthalpy and density. The two transport properties are the dynamic viscosity and the surface tension which has been previously implemented in MATLAB and is explained further in chapter 2.1.6 [Pálsson, 2011a].

3.2 Single Phase Flow

Single phase flow occurs when only one phase is present at a particular point in the well. In this case it can be either liquid or dry steam. The model calculates the mass fraction of steam at each point it chooses and converts to two phase flow simulation if the flow quality is between 0 and 1. The variables needed for the single phase simulation are u , P , h and the parameter ρ which can be derived from P and h .

3.2.1 The continuity equation

The continuity equation describes the transport of conserved quantity, in this case conservation of mass.

$$\frac{d}{dz}(\dot{m}) = 0 \quad (3.1)$$

In this model the diameter of the pipe is assumed to be constant, thus allowing equation (3.1) to be written in terms of density, cross sectional area of the pipe and the fluid velocity as

$$\frac{d}{dz}(\rho u) = 0 \quad (3.2)$$

3.2.2 The energy equation

The energy equation is derived from the first law of thermodynamics. The equation is divided into four parts, in the same order as listed below:

1. Kinetic part
2. Change in enthalpy per unit length
3. Gravitational potential energy
4. Heat loss per unit length

$$\dot{m}u \frac{du}{dz} + \dot{m} \frac{dh}{dz} + \dot{m}g + \dot{Q} = 0 \quad (3.3)$$

3.2.3 The momentum equation

The momentum equation is divided into four parts divided in the same order as listed below:

1. Change in inertia per unit length

3 Modeling Method

2. Pressure changes per unit length
3. Hydrostatic pressure gradient
4. Head loss

$$\rho u \frac{du}{dz} + \frac{dp}{dz} + \rho g + \frac{\rho f}{2d} |u|u = 0 \quad (3.4)$$

3.2.4 A system of equations

The equations in the last three subsections can be assembled in a matrix form. The matrix can be solved by using numerical integration which is explained later in this chapter.

$$\begin{bmatrix} \rho & u \frac{\partial \rho}{\partial p} & u \frac{\partial \rho}{\partial h} \\ \dot{m}u & 0 & \dot{m} \\ \rho u & 1 & 0 \end{bmatrix} \frac{d}{dz} \begin{bmatrix} u \\ p \\ h \end{bmatrix} + \begin{bmatrix} 0 \\ \dot{m}g + \dot{Q} \\ \rho g + \frac{\rho f}{2d} |u|u \end{bmatrix} = \begin{bmatrix} 0 \\ 0 \\ 0 \end{bmatrix} \quad (3.5)$$

3.3 Two Phase Flow

As stated earlier in this chapter the two phase flow simulation obeys the same laws of physics as a single phase flow. However the three main equations continuity, momentum and energy will have to take both phases into consideration. The additional parameters are void fraction and mass fraction. There are now two velocities present, steam and liquid velocity. The liquid velocity is defined as

$$u_l = \frac{\dot{m}_l}{\rho_l A_l} \quad (3.6)$$

The gas, or steam velocity is defined as

$$u_g = \frac{\dot{m}_g}{\rho_g A_g} \quad (3.7)$$

x is the quality or mass fraction of the gas in the mixture and is expressed in equation

3.8

$$x = \frac{h - h_l}{h_g - h_l} \quad (3.8)$$

3.3.1 The continuity equation

For the case of two phase flow the continuity equation will consist of both phases, water and vapor.

In this model the diameter of the pipe is constant and the equation can be written as

$$0 = \frac{d}{dz} (\dot{m}_l + \dot{m}_g) = \frac{d}{dz} (\rho_l u_l A_l + \rho_g u_g A_g) \quad (3.9)$$

Where α is the liquid/gas hold up or void fraction. This model assumes constant diameter so the continuity equation can be written as 3.10 [Pálsson, 2011a]

$$\frac{d}{dz} (\rho_l u_l (1 - \alpha) + \rho_g u_g \alpha) = 0 \quad (3.10)$$

$$\alpha = \frac{A_g}{A} \quad (3.11)$$

In the final equation u is introduced in place of the actual velocities

$$\frac{d}{dz} (\rho_l (1 - x) u + \rho_l x u) = 0 \quad (3.12)$$

$$\frac{d}{dz} (\rho_l u) = 0 \quad (3.13)$$

where u is defined in equation 3.14

$$u = \frac{\dot{m}}{\rho_l A} \quad (3.14)$$

3.3.2 The energy equation

The energy equation for two phase flow can be written as

$$\frac{d}{dz} \left(m_l \left(\frac{u_l^2}{2} + gz + h_l \right) + m_g \left(\frac{u_g^2}{2} + gz + h_g \right) + \dot{Q} \right) = 0 \quad (3.15)$$

3 Modeling Method

Next, the factor γ is introduced

$$\gamma = \frac{(1-x)^3}{(1-\alpha)^2} + \frac{\rho_l^2 x^3}{\rho_g^2 \alpha^2} \quad (3.16)$$

and finally the equation becomes

$$\gamma u \frac{du}{dz} + \frac{u^2}{2} \frac{\partial \gamma}{\partial p} \frac{dp}{dz} + \left(1 + \frac{u^2}{2} \frac{\partial \gamma}{\partial h}\right) \frac{dh}{dz} + g + \frac{\dot{Q}}{\dot{m}} = 0 \quad (3.17)$$

3.3.3 Momentum equation

The momentum equation for two phase flow is considerably more complicated than single phase flow equation. The equation has to account for the different phase velocities for the inertia part, the gravity part has to be an averaged value with respect to the void fraction

$$\rho_\alpha = (1-\alpha) \rho_l + \alpha \rho_g \quad (3.18)$$

Thus, the momentum equation for two phase flow becomes

$$\frac{d}{dz} (\dot{m}_l u_l + \dot{m}_g u_g) + A \frac{dp}{dz} + ((1-\alpha) \rho_l + \alpha \rho_g) g A + \Phi^2 \frac{\rho_l f A}{2d} u^2 = 0 \quad (3.19)$$

Where Φ is a correction factor for frictional pressure loss and f is the friction factor that will be described later in this chapter. To simplify the momentum equations parameter η is introduced

$$\eta = \frac{(1-x)^2}{1-\alpha} + \frac{\rho_l x^2}{\rho_g \alpha} \quad (3.20)$$

And finally the momentum equation can be written as 3.21

$$\eta \rho_l u \frac{du}{dz} + \left(1 + \rho_l u^2 \frac{\partial \eta}{\partial p} + \eta u^2 \frac{\partial \rho_l}{\partial p}\right) \frac{dp}{dz} + \rho_l u^2 \frac{\partial \eta}{\partial h} \frac{dh}{dz} + ((1-\alpha) \rho_l + \alpha \rho_g g) + \frac{\Phi^2 \rho_l f}{2d} u^2 = 0 \quad (3.21)$$

3.3.4 A system of equations

As for the single phase flow, the three governing equation can be assembled to matrix form that can be solved either by finite difference method or numerical integration from well bottom to the top.

$$\begin{aligned}
 & \begin{bmatrix} \rho_l & u \frac{\partial \rho_l}{\partial p} & 0 \\ \gamma u & \frac{u^2}{2} \frac{\partial \gamma}{\partial p} & \left(1 + \frac{u^2}{2} \frac{\partial \gamma}{\partial h}\right) \\ \eta \rho_l u & \left(1 + \rho_l u^2 \frac{\partial \eta}{\partial p} + \eta u^2 \frac{\partial \rho_l}{\partial p}\right) & \rho_l u^2 \frac{\partial \eta}{\partial h} \end{bmatrix} \frac{d}{dz} \begin{bmatrix} u \\ p \\ h \end{bmatrix} \\
 & + \begin{bmatrix} 0 \\ g + \frac{\dot{Q}}{m} \\ ((1 - \alpha) \rho_l + \alpha \rho_g g) + \frac{\Phi^2 \rho_l f}{2d} u^2 \end{bmatrix} = \begin{bmatrix} 0 \\ 0 \\ 0 \end{bmatrix} \quad (3.22)
 \end{aligned}$$

3.4 Slip ratio and void fraction correlations

Many different correlations for void fractions have been proposed. These correlations are derived from series of experiments, however they are most often limited to the experimental conditions they were carried out at. Equation 3.23 is a general equation of the void fraction, α . The no slip model (NS) is the most simple of void fraction models. It assumes that the water and steam move at the same velocity, hence the ratio of velocities, S is equal to one.

$$\alpha = \frac{\frac{x}{\rho_g}}{\frac{x}{\rho_g} + \frac{1-x}{\rho_l} S} \quad (3.23)$$

The slip ratio is defined as

$$S = \frac{u_g}{u_l} \quad (3.24)$$

Where u_g and u_l are the velocities of gas and liquid.

Lockhart Martinelli (1949) is one of the most widely used model today.

$$\alpha = \left[1 + 0.28 \left(\frac{1-x}{x} \right)^{0.64} \left(\frac{\rho_g}{\rho_l} \right)^{0.36} \left(\frac{\mu_l}{\mu_g} \right)^{0.07} \right]^{-1} \quad (3.25)$$

In order of age, void fraction models tested in the model process are listed here below.

Zivi(1964)

$$\alpha = \left[1 + \left(\frac{1-x}{x} \right) \left(\frac{\rho_g}{\rho_l} \right)^{0.67} \right]^{-1} \quad (3.26)$$

3 Modeling Method

Thom(1964)

$$\alpha = \left[1 + \left(\frac{1-x}{x} \right) \left(\frac{\rho_g}{\rho_l} \right)^{0.89} \left(\frac{\mu_l}{\mu_g} \right)^{0.18} \right]^{-1} \quad (3.27)$$

Baroczy(1966)

$$\alpha = \left[1 + \left(\frac{1-x}{x} \right)^{0.74} \left(\frac{\rho_g}{\rho_l} \right)^{0.65} \left(\frac{\mu_l}{\mu_g} \right)^{0.13} \right]^{-1} \quad (3.28)$$

Smith(1969)

$$\alpha = \left[1 + A_{SM} \left(\frac{1-x}{x} \right) \left(\frac{\rho_g}{\rho_l} \right) \right]^{-1} \quad (3.29)$$

Where A_{sm} is

$$A_{sm} = 0.4 + 0.6 \sqrt{\left[\frac{\rho_l}{\rho_g} + 0.4 \left(\frac{1-x}{x} \right) \right] / \left[1 + 0.4 \left(\frac{1-x}{x} \right) \right]} \quad (3.30)$$

Chisholm(1973)

$$\alpha = \left[1 + \sqrt{1 - x \left(1 - \frac{\rho_l}{\rho_g} \right)} \left(\frac{1-x}{x} \right) \left(\frac{\rho_g}{\rho_l} \right) \right]^{-1} \quad (3.31)$$

3.5 Friction factor

There are multiple methods of evaluating the friction factor. In this case both Colebrooke-White and Blasius were tested. The Colebrooke-White was assumed to be too sensitive to wall roughness so it was decided to use the Blasius method. It assumes that the walls are smooth, however it is very difficult to measure wall roughness in geothermal wells due to scaling. The friction factor, f is defined in equation 3.32 [Wallis, 1969]

$$f = \frac{0.316}{Re^{1/4}} \quad (3.32)$$

3.6 Friction correction factors

Friedel correction approximation is used to estimate the friction correction factor. The approximation includes both the gravity effect by the Froude number and the effect of surface tension addressed in the Weber number.

$$\Phi^2 = E + \frac{3.24FH}{Fr^{0.045}We^{0.035}} \quad (3.33)$$

$$E = (1 - x^2) + x^2 \frac{\rho_l}{\rho_g} \frac{f_g}{f_l} \quad (3.34)$$

f_l and f_g are two alternative friction factors based on the Reynolds number of each phase.

$$f_l = \frac{0.316}{Re_l^{1/4}} \quad (3.35)$$

and

$$f_g = \frac{0.316}{Re_g^{1/4}} \quad (3.36)$$

$$F = x^{0.78} (1 - x^2)^{0.24} \quad (3.37)$$

$$H = \left(\frac{\rho_l}{\rho_g} \right)^{0.91} \left(\frac{\nu_g}{\nu_l} \right)^{0.19} \left(1 - \frac{\rho_g}{\rho_l} \right)^{0.7} \quad (3.38)$$

$$Fr = \frac{\rho_l^2 u^2}{g \rho_m^2 d} \quad (3.39)$$

$$We = \frac{\rho_l^2 u^2 d}{\sigma \rho_m^2} \quad (3.40)$$

where the surface tension is defined as

$$\sigma = 0.2358 \left(1 - \frac{T}{T_c} \right)^{1.256} \left(1 - 0.625 \left(1 - \frac{T}{T_c} \right) \right) \quad (3.41)$$

3 Modeling Method

The mean density, ρ_m is defined in equation 3.42

$$\frac{1}{\rho_m} = \frac{x}{\rho_g} + \frac{1-x}{\rho_l} \quad (3.42)$$

$$Re_g = \frac{\rho_g u d}{\mu_g} \quad (3.43)$$

$$Re_l = \frac{\rho_l u d}{\mu_l} \quad (3.44)$$

3.7 Numerical Integration

As said before numerical integration is used to solve equations 3.22 and 3.5 over the production casings length. The equation is solved in MATLAB using a built in function called ode23. This function is an implementation of an explicit Runge Kutta (2,3) pair of Bogacki and Shampine method [Mathworks, 2012]. The function evaluates pressure, enthalpy and change in velocity at given locations along the well casing.

4 Measured data

For a data fitting analysis to be accurate it is necessary to have access to a reliable set of data. Insufficient data can have negative impact on the results.

Measurements Icelandic Geosurvey performs well measurements for the Icelandic energy companies. Icelandic Geosurvey (ÍSOR-Íslenskar orkurannsóknir) is a state owned company which possesses a team of expert and necessary measuring equipment. Measurements are carried out when the well is open and flowing. Measurements are not performed on wells when they are connected to the production plant. In this report it is assumed that the well has been open long enough to reach equilibrium.

Pressure and temperature Pressure measurements are performed with the K10 geothermal logging tool. This equipment which is manufactured by Kluster Company can operate downhole for up to 6 hours at 300°C . The battery equipment in the tool is protected inside a pressure housing. The pressure transducers sense the well pressure through a capillary tube and the temperature with an external fast response resistive temperature device made of platinum. The tool has a built in memory that logs data to a flash memory object [Kluster, 2012]. The tool is lowered into the well on a string, however the string elongates in the high temperature thus increasing the uncertainty in the measurements.

4.0.1 Mass Flow

It is complicated or to get a accurate mass flow measurement in a geothermal well. Up until today there have been two methods or approaches that are most widely used. The Russell James method and tracer flow testing (TFT).

Russell James method

This method can be used on two phase and dry steam wells. The method is based on reaching critical pressure by making the flow reach sonic velocity. This is also known as choking, hence choked flow when the mass flow cannot be increased. The critical pressure is measured and flow of water from the silencer is also measured in a V-notch. From these two values it is possible to calculate, total flow and quality of the steam in the well [Gunnlaugsson, 2007]. The estimation formula is described in equation 4.1

$$\dot{m} = K A \frac{P_c^m}{h_n} \quad (4.1)$$

Where P_c is the critical pressure in bar-a, A is the radius and $m=0.96$, $n=1.102$ and $K=1835000$ are constants.

Tracer flow testing

Tracer flow testing (*TFT*) is more accurate method than the Russell James. It is however more time consuming and requires a lab, however it can be used without disconnecting the hole from production [Gunnlaugsson, 2007]. It requires accurately measured rates of liquid and vapor-phase tracers that are injected into the two phase stream. After that, samples are collected from separators downstream to ensure that the tracers are equally distributed in each phase. The samples are analyzed in a lab where tracer content is measured. The mass flow rate of each phase is calculated based on injection rate of each tracer and measured concentration from the samples. The mass rate of liquid Q_l and Q_s is written as in equation 4.2 [Hirtz et al, 2001].

$$\dot{m}_{l,s} = \frac{\dot{m}_T}{C_T} \quad (4.2)$$

where

$\dot{m}_{l,s}$ are mass flow rate of liquid and steam respectively

\dot{m}_T is the tracer injection mass rate kg/s

C_T is the tracer concentration by weight

In the measurement process there are a few factors mentioned that should be kept in mind during the process

1. Measurements should be carried out when the well is flowing.
2. Pressure, temperature and mass flow should all be measured at the same time.
3. Report with the measurements should state if the measurement was carried down hole or up.
4. The measurement tools should be calibrated before and uncertainty of the equipment should be stated with the data analysis.
5. The measurement tools are lowered in to the well on a string. The tool string should be measured before and after since it will elongate in the well due to high temperature to be able to evaluate the uncertainty in the depth measurement.
6. Well profile, casing program and direction of the drilling should be mentioned in the reports which accompany the data.

4.1 Data source

The energy companies which granted access to data for this project are HS Energy and Reykjavik Energy.

Einar Gunnlaugsson and Gunnar Gunnarsson department manager and specialist at Reykjavik Energy provided data for the author used in this modeling. The first set of data which did not include the actual measurement results where gathered in September 2011, more data was aquired in May 2012. The measurements come from wells at the Hellisheiði area which is located in the southern part of the Hengill geothermal area. At Hellisheiði, Reykjavík Energy operates electricity and district heating plant with a capacity of $303MW_e$ and $133MW_{th}$. Hellisheiði is located 25 km from the capital, Reykjavík.

Albert Albertsson, Geir Þórólfsson vice president and project manager at HS Energy granted access to both areas it operates at, Reykjanes and Svartsengi. The data was gathered in September 2012. At Reykjanes, HS Energy operates $100MW_e$ power plant and $75MW_e$ at Svartsengi. Reykjanes and Svartsengi are two separated geothermal reservoirs at the Reykjanes peninsula.

4.2 Data

All measurement data used in this assignment were collected when the wells were open and flowing. There were more wells that were tested but the measurements and other data around it proved to be unsatisfactory due to lack of adequate information on the well profile or inconsistency in measurements.

Wells from Reykjavík Energy				
	HE-5	HE-20	HE-44	HE-48
Depth of production casing [m]	791	687	836	829
Wellhead Pressure [bara]	19	12.5	15.3	14.5
Pressure at production casing bottom [bara]	47.5	30.14	30.17	36.48
Mass flow [kg/s]	49.0	33.33	33	39.2
Enthalpy [kJ/kg]	1194	1053	1084	1072
Inner diameter [m]	0.22	0.22	0.315	0.315

Wells from HS Energy			
	RN-11	RN-12	SV-21
Depth of production casing [m]	689	687	839
Wellhead Pressure [bara]	41	40.5	14.5
Pressure at production casing bottom [bara]	59.9	58	39
Mass flow [kg/s]	50	49	70
Enthalpy [kJ/kg]	1300	1300	1030
Inner diameter [m]	0.300	0.300	0.315

5 Results

In the introduction chapter it was stated that the purpose of this model was to use a previously known no slip model for calculating pressure drop in a two phase flow and compare the results with measured data from a geothermal well by calculating the actual slip ratios present in the well. The following chapter reveals the results from modeling work based on previous chapters.

5.1 Comparison of different flow models for each well

In this section the no slip model and six other void fraction models are compared to the measured data. The pressure drop models show a relatively wide spread in their predictions. The absolute error was evaluated as referred in equation 5.1.

$$\text{Absolute Error} = | \text{predicted value} - \text{measured value} | \quad (5.1)$$

The results are shown in the tables and figures to follow. First the well head pressure which each model yielded and then the absolute error from measured well head pressure with a calculated average error. Figures 5.1 through 5.4 show the results from the modeling and the measured values on graphs where the pressure is plotted versus depth to the production casing.

5 Results

Wellhead pressure bar-a.							
	HE-5	HE-20	HE-44	HE-48	RN-11	RN-12	SV-21
Measured wellhead pressure	19	11.5	15.3	14.5	39.5	40.0	13.5
NS	16.58	15.3	14.2	13.7	43.8	46.2	14.9
Thom (1964)	8.00	11.14	9.10	9.6	35.3	41.3	9.6
Lockhart Martinelli (1949)	8.03	8.4	9.08	13.3	41.8	47.8	9.9
Smith	6.578	10.21	8.0	11.4	35.3	42.3	8.3
Baroczy	19.1	7.0	7.0	10.2	34	41.2	6.8
Chisholm	11.50	8.06	7.5	6.0	35.8	42.7	8.3
Zivi	18.28	14	16.3	20.2	38.7	50.8	17.3

Absolute Error in Wellhead pressure bar-a.							
	HE-5	HE-20	HE-44	HE-48	RN-11	RN-12	SV-21
NS	2.42	3.80	1.10	0.80	4.30	6.20	1.40
Thom	11.10	0.36	6.20	4.90	4.20	1.30	3.90
Lockhart Martinelli	10.99	3.10	6.20	1.20	2.30	7.80	3.60
Smith	12.42	1.29	7.30	3.10	4.20	2.30	5.20
Baroczy	0.10	4.50	8.30	4.30	5.50	1.20	6.70
Chisholm	7.50	3.44	7.80	8.50	3.70	2.70	5.20
Zivi	0.72	2.50	1.00	5.70	0.80	10.80	3.80

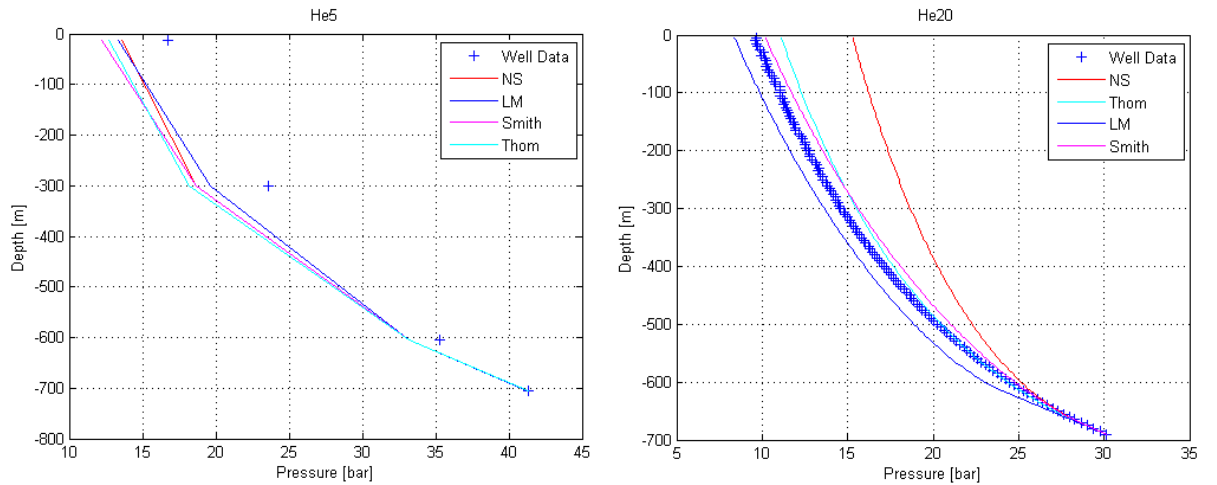


Figure 5.1: Simulations of wells HE-5 (left) and HE-20 (right) from the bottom of the production casing to the well top.

On the left side of figure 5.1 the results of modeling for well HE-5 are presented. The Lockhart-Martinelli model yielded the best result with an absolute error of 0.67 bar and the Baroczy model the worst with 12.75 bar from the measured value. Although there were two sets of data available for this well, they both yield a similarly bad result with only 4 measurement points down to the production casing bottom indicating that the quality of the measurement process can be questioned.

5.1 Comparison of different flow models for each well

Results from well HE-20 modeling are presented on the right side of figure 5.1. The sample data for this well consisted of 138 measurement points. The well is liquid dominated with an estimated enthalpy of 1053 kJ/kg. The well depth was corrected for the directional drilling, however the no slip model delivered the worst results with an error of 3.80 bar and Thom the best at 0.36 bar.

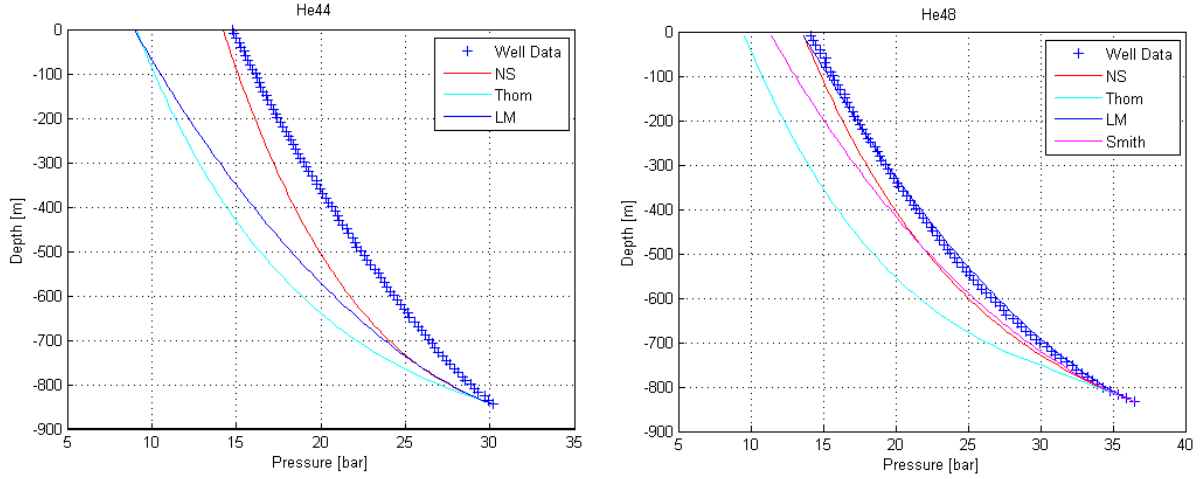


Figure 5.2: Simulations of wells HE-44 (left) and HE-48 (right) from the bottom of the production casing to the well top.

On the left side of figure 5.2 the results from simulation of well HE-44 are presented. HE-44 is a directionally drilled liquid dominated well with an estimated enthalpy of 1084 kJ/kg. There are 87 measurement points to the production casing bottom. The Zivi model gave the best result with an absolute error of 1.03 bar making the no slip model the runner up with an error of 1.08 bar. Chisholm model gave the worst result with an error of 7.20 kJ/kg from measured well head pressure.

Results from simulation of well HE-48 are presented on the right side. Well HE-48 is a liquid dominated well with an enthalpy of 1072 kJ/kg and directionally drilled. There were 87 measuring points in the data set. The no slip model delivered results that were closest to the measured value with an error of 0.82 bar. Chisholm model gave the worst results with an absolute error of 8.46 bar.

5 Results

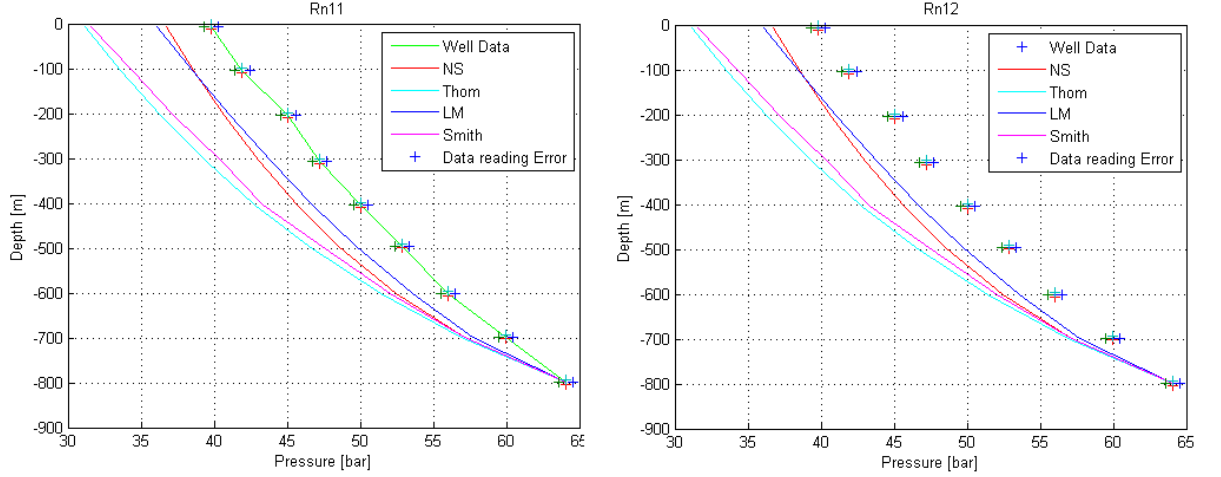


Figure 5.3: Simulations of wells Rn-11 (left) and Rn-12 (right) from the bottom of the production casing to the well top. In addition to the simulation results and measurement a data reading error was evaluated due to data reading accuracy on the graphs provided by HS energy. The error was estimated as ± 1 bar and ± 10 m

For the two wells shown on figure 5.3 the measured well head pressure has a data reading error due to lack of access to the original numerical data. The error was estimated as ± 1 bar and ± 10 m

Simulations for well RN-11 is on the left side of figure 5.3. The well has an estimated enthalpy of 1300 kJ/kg. Zivi model gave the best result with an error of 2.11 bar from the measured value with the no slip model at 2.79 bar.

Modeling of well RN-12 is shown on the right side of figure 5.3. The well has an estimated value of 1300 kJ/kg. Zivi and the no slip model gave a similar result with 1.6 bar error

On figure 5.4 results from simulation of well SV-21 is presented. The well is a liquid dominated with an estimated well enthalpy of 1030 kJ/kg. The well has 8 measurement points down to the production casing. No slip model delivered the best results for this well with an error of 0.2 bar.

For all the wells combined, the no slip model returned the best results with an average absolute error of 1.82 bar. The Lockhart Martinelli model was the runner up with an average error of 3.12 bar.

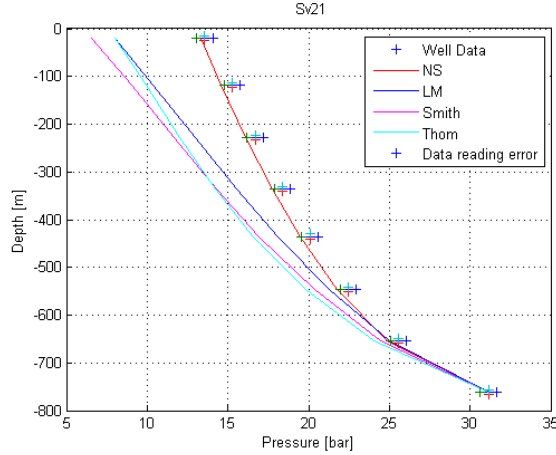


Figure 5.4: Simulations of wells SV-21 from the bottom of the production casing to the well top. In addition to the simulation results and measurement a data reading error was evaluated due to data reading accuracy on the graphs provided by HS energy. The error was estimated as ± 1 bar and ± 10 m

5.2 Well head pressure and its sensitivity to changes on slip ratio

It is interesting to take a look at what changes on slip ratio will have on the well head pressure. The results are introduced in figures 5.5 to 5.8. For each 10% change in slip ratio the calculated well head pressure lowers by 3 – 4%.

In figure 5.5 the measured values of well HE-5 on the left do not cross with the simulation results. However for well HE-20 on the right side of the figure 7 of the total of 11 points are within the measurement error region. The data for HE-20 are considered more reliable due to amount of measurement points compared to well HE-5 which had very few.

For both the wells in figure 5.6 this analysis delivered 6 different slip ratios within the measurement error margin. These two wells had relatively reliable data compared to well HE-5.

Wells RN-11 and RN-12 have higher enthalpy than other wells. The model seem not perform as well on well with higher steam content. All of the simulated points are outside the measurement error margin.

5 Results

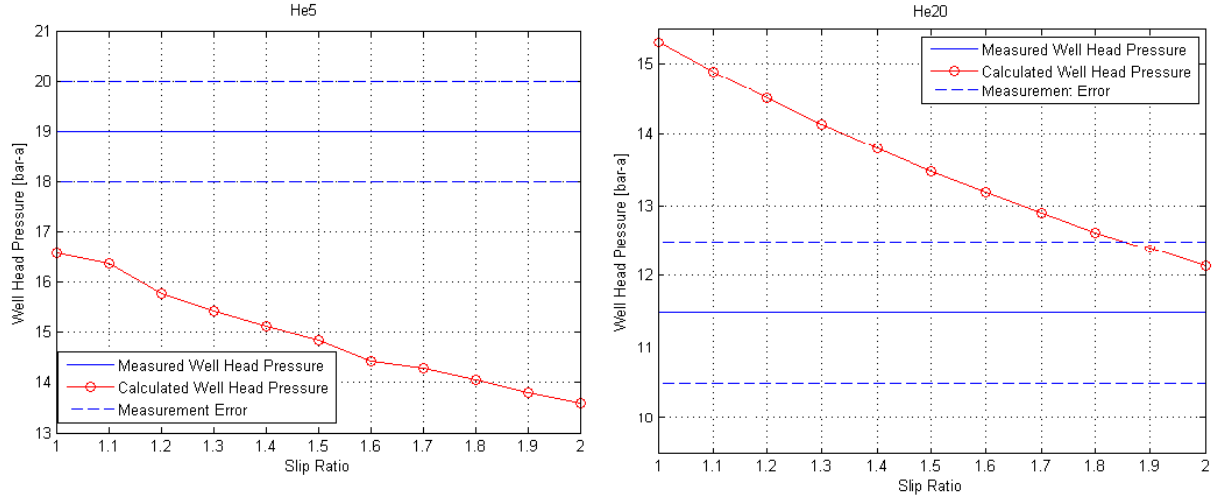


Figure 5.5: Simulated well head pressure changes when the slip ratio input value is changed for wells HE-5 (left) and HE-20 (right). The red line represents the simulated value of wellhead pressure, the blue line is value for measured well head pressure and the blue dotted lines represent the measurement uncertainty evaluated as ± 1 bar for each $\pm m$.

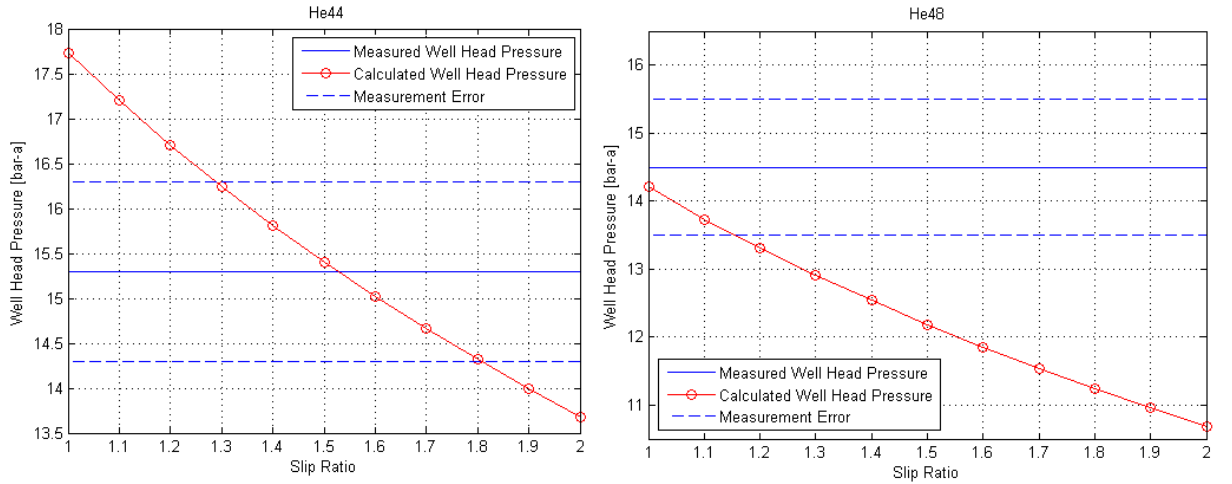


Figure 5.6: Simulated well head pressure changes when the slip ratio input value is changed for wells HE-44 (left) and HE-48 (right). The red line represents the simulated value of wellhead pressure, the blue line is value for measured well head pressure and the blue dotted lines represent the measurement uncertainty evaluated as ± 1 bar for each $\pm m$.

Well SV-21 is a liquid dominated well. The slip ratio for this well is closest to the no slip model.

5.2 Well head pressure and its sensitivity to changes on slip ratio

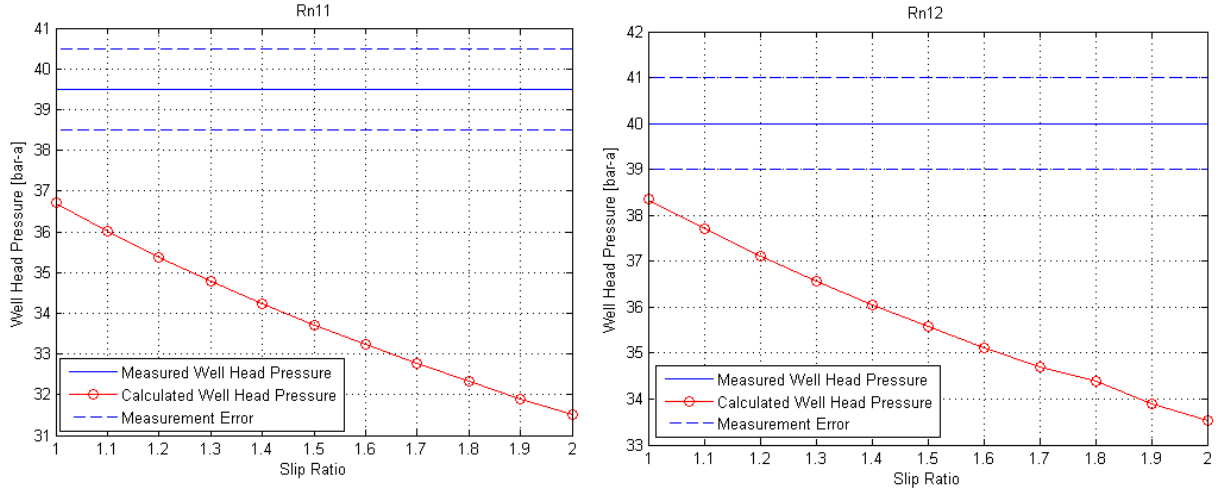


Figure 5.7: Simulated well head pressure changes when the slip ratio input value is changed for wells RN-11 (left) and RN-12 (right). The red line represents the simulated value of wellhead pressure, the blue line is value for measured well head pressure and the blue dotted lines represent the measurement uncertainty evaluated as ± 1 bar for each ± 1 m.

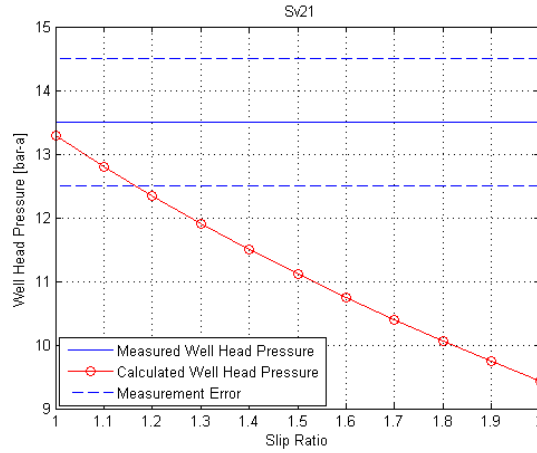


Figure 5.8: Simulated well head pressure changes when the slip ratio input value is changed for well SV-21. The red line represents the simulated value of wellhead pressure, the blue line is value for measured well head pressure and the blue dotted lines represent the measurement uncertainty evaluated as ± 1 bar for each ± 1 m.

5.3 Slip ratio calculation on different depths in the well

One aspect to this project was to map the distribution of slip ratio at different depths in the wells. The slip ratio is defined as in equation (3.24). Instead of using known void fraction correlations to calculate the pressure drop, the model was given the pressure drop according to the data. The model then calculated the corresponding slip ratio to that particular pressure value at depth each hundred meters. Note that there is no slip ratio available below the flashing zone due to the flow being only liquid.

The result can be seen on figure (5.9).

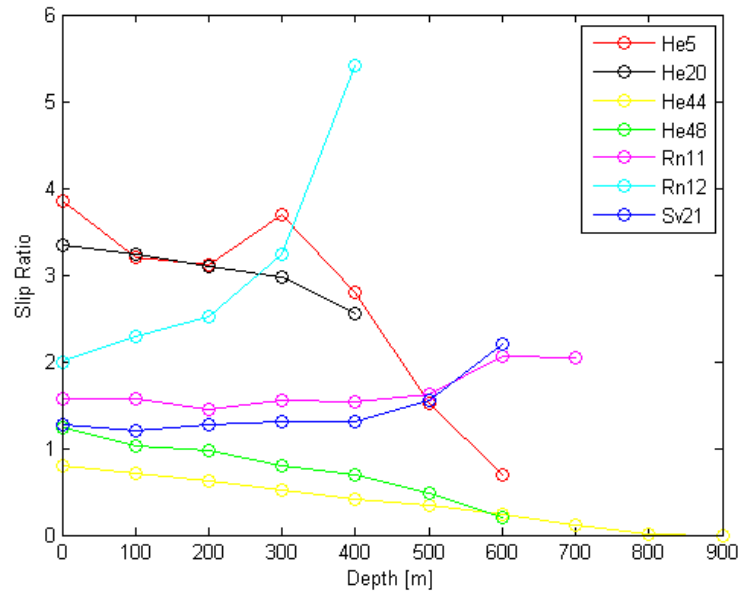


Figure 5.9: Calculations of slip ratio at known locations in the wells where the well head pressure is known.

It is a recognized fact that the steam will move at the same velocity or faster than liquid when the pressure decreases. However, figure 5.9 points otherwise. For wells RN-11, RN-12 and SV-21 the slip ratio increases with depth, hence the velocity of the steam will decrease with declining pressure, which is not possible. The slip ratios for well HE-44 are always below 1, indicating that the liquid phase is moving faster at all the sample points in the well, HE-44 is similar with two sample points near the wellhead where the slip ratio is a little over 1, but below 1 on all other locations in the sample points. Wells HE-5 and HE-20 are the only two with the

5.3 Slip ratio calculation on different depths in the well

slip ratio distribution that points in the right direction, excluding one anomaly at 300 m depth in well HE-5.

From this results of backward calculations it has been confirmed that the measurement data used in this modeling procedure is not accurate enough to be used to improve pressure drop models for geothermal wells.

It is a very challenging subject to measure pressure and mass flow in geothermal wells. The measurement technique was described in details in chapter 4.2. It has been mentioned earlier that the mass flow measurement are not carried out at the same time as the pressure/temperature measurements and that the enthalpy is an estimated parameter. Hence, the next step was to do a sensitivity analysis on how mass flow measurement affects the calculated well head pressure and demonstrate the importance of carrying measurements out carefully and preferably at the same time.

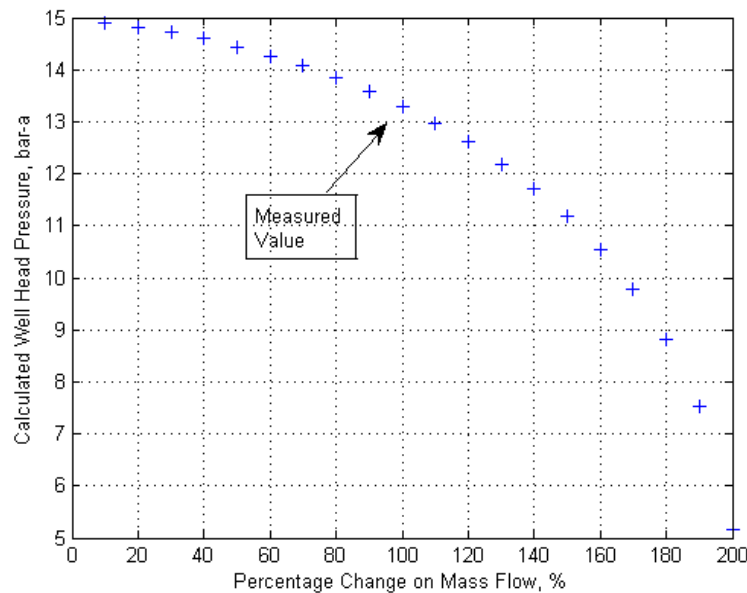


Figure 5.10: The figure illustrates the effects the measured input value of mass flow on well head pressure calculations on well SV-21. When the mass flow changes by 10%, the well head pressure changes by 1-2%.

Figure (5.10) shows the connection between the mass flow measurement input and the result of wellhead pressure calculations from the model. If the mass flow is decreased the wellhead pressure increases. For all the wells, excluding well HE-20 the mass flow might have been measured to low, also the enthalpy estimate can effect the results, lower enthalpy will yield lower well head pressure.

6 Conclusions

The main objective of this project was to conduct a model which simulated two phase flow in geothermal wells from the bottom to the top. Then use that model to adjust slip ratio values in order to fit measured data. The initial idea was to figure out some kind of optimal slip ratio or correlation that would give better results than existing models. Previous models have been estimated from experiments that have been carried out under well defined circumstances that may not apply to geothermal wells due their much larger dimensions.

Orkuveita Reykjavíkur and HS Orka provided measured data for the the author which is used in the analysis. The slip ratio analysis revealed that the data used for comparison is not accurate enough to use for this purpose. A possible reason may be the fact that the pressure and mass flow measurements are not carried out at the same time and sometimes with weeks in between measuring times. Furthermore the mass flow fluctuates quite a bit which adds to the problem. Other reasons why this analysis did not go as initially planned is that the mass flow is considered constant, heat losses are neglected and the well walls are considered smooth. The roughness of walls is almost impossible to measure due to conditions in the well. The well walls are considered smooth in the model and also all heat losses to the surrounding rock are neglected.

Since the slip ratio analysis did not go as planned and due to the uncertainty regarding the data it was decided to take a look at well known void fraction correlations and compare them to the data set and assess their performance against the simple no slip model. The error in the measurement was estimated to be at least $+/- 1$ bar and 10m in depth. That analysis concluded that the no slip model was an acceptable choice, with 1.40 bar error compared to the runner up, Lockhart Martinelli model showing a 3.60 bar average error. In addition, compared to more complicated correlations, the no slip model had the shortest execution time.

To be able to improve this type of modeling it is important to figure out new void fraction correlations that can be applied to geothermal wells. These correlation will require a wide range of data from many different wells over a long period of time. This is an expensive procedure and would require cooperative between many different parties, the energy companies, measurement experts and the universities. Such

6 Conclusions

data collection would pay off in the long haul since these pressure drop models can assist in the selection of diameters of geothermal wells, thus potentially decrease cost of drilling. There are a few things that should be introduced in the measurement process, that is to measure the pressure, temperature and mass flow at the same time and increase the number of measurement points since there is lack of that in many data sets. Also, easier access to data could also bring great progress to geothermal well modeling since lack of quality data is hindering progress in that area of expertise.

Bibliography

- Dipippo, R. 2008. *Geothermal power plants : principles, applications, case studies and environmental impact*. Oxford. Butterworth Heinemann, 2nd Edition. p. 54-57.
- Eggertsson, H, Thorsteinsson, Í, Ketilsson, J, Loftsdóttir, Á. 2011. *Energy statistics 2010 (Orkutölur 2010)*. Orkustofnun.
- Gunnlaugsson, E., Oddsdóttir, A.L 2009. *Hellisheidi - Gufuborholur 2007: Afl, vatnsborð og vinnsla* Reykjavik Energy.
- Haraldsson, I, Ketilsson, J. 2010. *Geothermal utilization for electricity production and direct use to the year 2009 (Jarðhitanoftun til raforkuvinnslu og beinna nota til ársins 2009.)* Orkustofnun. OS2010-2
- Hirtz, P. N., Kunzman, R. J., Broaddus, M. L., and Barbitta, J. A. 2001. *Developments in tracer flow testing for geothermal production engineering*. Geothermics 30, p.727-745
- Hole, H. 2008. *Geothermal Well Design, Casing and Wellhead*. Petroleum Engineering Summer School. Dubrovnik, Croatia. Workshop 26
- Ingason, K, Matthíasson, M. 2006. *Drilling cost of high temperature wells (Kostnaður við borun og frágang háhitahola. In Icelandic)*. Málþing jarðhitafélags Íslands. (Icelandic Geothermal association). February 2006.
- Jóhannesson, H, Sæmundsson, K. 2002. *Geothermal map of Iceland*
- Kluster Company, 2012. *Kuster K10 Geothermal PTS Memory* [http://www.kusterco.com/pdfs/2012/Probe KusterK10GeothermalPTS.pdf](http://www.kusterco.com/pdfs/2012/Probe%20KusterK10GeothermalPTS.pdf). File retrieved 9.july 2012.
- Mathworks. 2012. *ode23, ode45, ode113, ode15s, ode23s, ode23t, ode23tb*. <http://www.mathworks.se/help/techdoc/ref/ode45.html> File Retrieved 9.august 2012
- Pálsson, H. 2011a. *Simulation of two phase flow in a geothermal well*. Lecture notes. University of Iceland.

BIBLIOGRAPHY

- Pálsson,H. 2011b.*Two phase flow regimes*. Lecture notes. University of Iceland.
- Thorhallsson, S. 2008.*Geothermal drilling and wellpumps* Presented at the workshop for Decision makers on direct heating use of geothermal resources in Asia. Organized by UNU GTP.
- Thorhallsson,S. 2011. *Geothermal boreholes*. Lecture notes. University of Iceland.
- Vijayarangan,B.R, Jayanti,S, Balakrishnan,A.R.2006.*Pressure drop studies on two phase flow in a uniformly heated vertival tube at pressure up to the critical point*. International Journal of Heat and Mass Transfer 50 (2007) 1879-1891.
- Wallis,G. B. 1969.*One-dimensional Two phase Flow*. New York: McGraw-Hill.
- Woldesemayat M.A, and Ghajar, A.J. 2006.*Comparison of void fraction correlations for different flow patterns in horizontal and upward inclined pipes*. International Journal of Multiphase Flow 33 (2007) 347-370.
- Zhao, X.2005. *Mechanistic-based models for slug flow in vertical pipes*. Ph.d thesis, Texas Tech University.